Applied Mathematics & Information Sciences
An International Journal

http://dx.doi.org/10.18576/amis/170320

Establishing the Coexistence of *Wolbachia*-Carrying and Wild *Aedes aegypti* Populations by Feedback Linearization

*Antone dos Santos Benedito**, *Claudia Pio Ferreira and Helenice de Oliveira Florentino*

Departamento de Biodiversidade e Bioestatística, Instituto de Biociências (IBB), Universidade Estadual Paulista Júlio de Mesquita Filho (UNESP), 18618-689, Botucatu-SP, Brazil

Received: 12 Feb. 2023, Revised: 2 Apr. 2023, Accepted: 22 Apr. 2023
Published online: 1 May 2023

Abstract: *Wolbachia*-based control for the reduction of arboviruses transmitted by *Aedes aegypti* mosquito is often designed to thoroughly wipe out the wild population replacing it by *Wolbachia*-carrying individuals. Overall, there has been no focus on plans looking for establishing the coexistence of these populations sharing the same locality. Holding repeated replacement interventions could lead us in a long-term to a possible eradication scenario for this species in its natural state. Nevertheless, annihilating species has been a subject of great controversy and qualms among conservative scientists, since there is no warranty of safeguarding the ecological balance and human welfare. Taking this into account, we explore the application of two non-classical techniques for optimal control proposition, Feedback (Exact) Linearization and Genetic Algorithm, to a system composed of *Wolbachia*-carrying and wild *Aedes aegypti* populations aiming to achieve the coexistence equilibrium. The Feedback Linearization technique is used to provide a control law by which one rules the releases of *Wolbachia*-carrying mosquitoes so that the system solution locally asymptotically stabilizes around the coexistence steady-state. In addition, the Genetic Algorithm is used to propose a control strategy to be introduced in a worst-case scenario, when the wild population is at the level of the carrying-capacity without the presence of *Wolbachia*-carrying mosquitoes. Remarkably, the presented strategy is very interesting because it consists in applying the control with higher intensity in the early days and fairly low as the solution approaches the coexistence equilibrium. Furthermore, the control can be temporarily interrupted, reducing the costs to zero for a considerable length of time.

Keywords: exact linearization, optimal control, ordinary differential equation, stability analysis

1 Introduction

The control of insect population through environmental-friendly techniques is an old subject of research that has been growing in importance within the context of agroecosystem and epidemiology [1,2], partly for the sake of resistance to pesticides arising in agricultural pests and human disease vectors worldwide [3,4,5]. Due to its broad geographic distribution and the ability to transmit several diseases, the *Aedes* mosquito is one of the main targets for vector control [6]. Among the arboviruses transmitted by this genus are Dengue, Yellow fever, Zika, Murray Valley, La Crosse, Chikungunya, and Rift Valley fever [7,8,9]. For most of them, an efficient and safe vaccine is not available yet, and although a lot of effort has been done to control the mosquito population, the current strategies are proving inadequate [10,11,12]. Several factors such as climate change, urbanization, connectivity, poverty, land use and land cover change, behavior, and chemical resistance of this mosquito are associated with the failure of vector control efforts [13,14,15].

Consequently, the idea of integrated intervention for insect-borne diseases is gaining attention. Focusing on Dengue and *Aedes* mosquito, for example, the identified bottlenecks are (i) assessment of current vector control tools and those under development, and (ii) how to combine the best vector control options with effective DENV vaccines [16]. In this context, a novel and promising control technique is based on the release of *Wolbachia*-carrying mosquitoes. While this endosymbiotic bacterium can be naturally found on *Aedes albopictus*, the presence of it on *Aedes aegypti* is still under debate [17]. *Wolbachia* is maternally inherited and has an astonishing capability to manipulate host reproduction. Four reproductive manipulation phenotypes are described as caused by this bacterium: cytoplasmic incompatibility, male killing, parthenogenesis induction,

* Corresponding author e-mail: antone.santos@unesp.br

and feminization [18]. All of them provide infected female hosts with a reproductive advantage relative to uninfected females. Artificial infection of mosquito *Aedes* is done by embryonic microinjection of *Wolbachia*-infected cytoplasm or *Wolbachia* purified from infected insect hosts, and more likely to be successful when the donor and recipient organisms are closely related. Before releasing *Wolbachia*-carrying mosquitoes on the field, the power of *Wolbachia* strains to generate viral blockage and its influence on host fitness have to be assessed [19].

Few mathematical models have addressed the suppression of both populations using some control technique [20,21], while many others explore the replacement of the wild *Aedes aegypti* population by *Wolbachia*-carrying individuals [22,23,24,25]. Holding repeated replacement interventions could lead us in a long-term to a possible eradication scenario for this species in its natural state. Nevertheless, annihilating species has been a subject of great controversy and qualms among conservative scientists, since there is no warranty of safeguarding the ecological balance and human welfare. To our knowledge, there is no work in the literature focusing on a coexistence scenario of both populations, since this is generally unstable when perfect maternal inheritance, unstructured panmictic host population, and high CI-driven competition are considered. Thus, we addressed the nonlinear model presented in [24] attempting to apply the feedback linearization technique in order to achieve the coexistence of *Wolbachia*-carrying and wild *Aedes aegypti* populations with a decreasing control effort.

The feedback linearization technique turns the dynamics of a nonlinear system into linear dynamics by means of nonlinear feedback of the states or outputs [26, 27]. One of its several applications is to provide a control law to "force" the local asymptotic stability of unstable steady states, which we intend to handle here. This methodology has been employed efficiently in several application fields such as ballistics, robotics, aeronautics, medicine, pharmacy, chemical industry, and others [26, 27]. Going further than [28] that already used this technique to *Aedes aegypti* population control, our paper presents the first research based on both feedback linearization technique and *Wolbachia* bacterium for that purpose.

In short, we propose in this work a biocontrol strategy based on *Wolbachia* to promote the coexistence of wild and *Wolbachia*-carrying *Aedes aegypti* mosquitoes. The feedback linearization technique applied to a dynamical system provides both a mathematical expression for a controller and the necessary conditions so that it can keep the intended coexistence. Depending on the wild population size, an extra control will be primarily required to provide an appropriate level where the usage of the feedback linearization control is effective.

This paper is organized as follows. Section 2 presents the model proposed by [24] for the mosquito population dynamics. Section 3 approaches the feedback linearization technique stressing the input-output type. In Section 4, the feedback linearization is applied to the model and a control law for the coexistence steady state is determined. Section 5 presents an optimization model to obtain an extra control to then implement effectively the control law. In addition, a genetic algorithm is proposed to solve the optimization model by reducing as much as possible both the application period and the total cost. Finally, computational results are discussed.

2 On the model dynamics

Let $F := F(t)$ and $W := W(t)$ be state variables describing respectively the number of *Wolbachia*-free and *Wolbachia*-carrying adult female mosquitoes at each time t. The interaction between the populations can be modeled by

$$\begin{aligned} \dot{F}(t) &= f_1\left(F(t), W(t)\right) \\ \dot{W}(t) &= f_2\left(F(t), W(t)\right) + u(t), \quad t > 0, \end{aligned} \tag{1}$$

where $u(t)$ is a non-negative function standing for the control (number of *Wolbachia*-carrying mosquitoes to be released on a day t at a target locality) [24]. The functions $f_i\left(F, W\right), i = 1, 2$, are defined as

$$\begin{aligned} f_1\left(F, W\right) &= \left(\phi_f - \tfrac{r_f}{K_f}(F + W)\right) F \left(\tfrac{F}{K_0} - 1\right) - \delta_f F, \\ f_2\left(F, W\right) &= \left(\phi_w - \tfrac{r_w}{K_w}(F + W)\right) W - \delta_w W, \end{aligned} \tag{2}$$

where ϕ_j, δ_j, $r_j = \phi_j - \delta_j$ (with $j = f, w$ corresponding, sequentially, to the *Wolbachia*-free and *Wolbachia*-carrying population) denote the natural birth and death rates of adult female mosquitoes in absence of the density dependence and the intrinsic growth rate of female mosquitoes in absence of the density dependence, respectively. In turn, K_f is a parameter related to the wild carrying capacity and K_w represents the *Wolbachia*-infected carrying capacity itself. The term $\left(\frac{F}{K_0} - 1\right)$, with K_0 associated to the wild population size when the infection frequency reaches its steady state, includes an undercrowding term on the recruitment of the *Wolbachia*-free population (which together with the others terms will model the *Allee-effect*) coming from the fact that only mating among *Wolbachia*-free mosquitoes produces *Wolbachia*-free offspring due to cytoplasmic incompatibility (CI). Therefore, when the uninfected population is small ($F < K_0$), few individuals will be recruited for the new generation, emulating the effect of CI which guarantees that only mating between uninfected mosquitoes produces viable eggs. Observe that this is not true for the female *Wolbachia*-carrying mosquitoes, which can mate with infected or uninfected male mosquitoes; thus, this term is not present on f_2. Furthermore, the

model considers both perfect/efficient maternal transmission and host reproductive manipulation (CI). Regarding equations (1) and (2), in the absence of control (i.e. $u(t) = 0,\ \forall t > 0$) and interaction between the populations (i.e. $f_1(F,0)$ and $f_2(0,W)$) the dynamics of F and W will be driven by a logistic equation and by a strong Allee-effect, respectively. Lastly, although the proposed model does not comprise explicitly the sterilizing effect on infected mosquitoes caused by the sperm-egg incompatibility, it reproduces the results obtained when CI is explicitly modeled [25].

Ignoring any control and considering $\phi_w < \phi_f$, $r_w < r_f$, $\delta_w > \delta_f$, $\phi_f > \delta_f$ and $\phi_w > \delta_w$ (which is biologically reasonable, since the first three inequalities mean that the bacteria impact negatively the infected mosquito fitness, and the two last ones are needed to ensure that birth overcomes death), the dynamical system (1) has five steady states $(\bar{F}, \bar{W})$:

a) the trivial one $(0,0)$, where both mosquito populations go to extinction, which is always unstable;
b) one nodal repeller $(K_b, 0)$ where $K_b > 0$ indicates the minimum viable population size of uninfected mosquitoes

$$K_b = \frac{r_f K_0 + \phi_f K_f - \sqrt{\Delta}}{2r_f}, \quad \text{where}$$

$$\Delta = (r_f K_0 + \phi_f K_f)^2 - 4 r_f K_0 K_f (\phi_f + \delta_f);$$

c) one saddle point (F_c, W_c) of unstable coexistence of both mosquito populations with

$$F_c = \frac{K_0\left[\phi_f\left(K_f - K_w\right) + \delta_f\left(K_f + K_w\right)\right]}{\phi_f\left(K_f - K_w\right) + \delta_f K_w},$$

$$\text{and} \quad W_c = K_w - F_c;$$

d) two nodal attractors $(0, K_w)$ and $(K_*, 0)$, where $K_* > K_f$ defines the carrying capacity of wild females, and

$$K_* = \frac{r_f K_0 + \phi_f K_f + \sqrt{\Delta}}{2r_f}.$$

Relying exclusively upon the initial conditions, just one of these steady states can be reached:

i. If $F(0) > K_b$ and $W(0) > 0$ then $(F(\infty), W(\infty)) = (K_*, 0)$. This steady state corresponds to the persistence of wild mosquitoes and extinction of *Wolbachia*-carriers.
ii. If $F(0) < K_b$ and $W(0) > 0$ then $(F(\infty), W(\infty)) = (0, K_w)$. This steady state corresponds to the persistence of *Wolbachia*-carriers and extinction of wild mosquitoes.

Observe that K_b depends on the birth and death rates and on the carrying capacities.

In [24], it is assumed that $K_w < K_f$, and a control strategy is used to bring the solution from $(K_*, 0)$ to $(0, K_w)$, but there was no intervention towards (F_c, W_c) due to its instability. With this in view, we want to find a control function to bring the solution of system (1) to this coexistence point, avoiding the total suppression of the wild *Aedes aegypti* population and assuring the permanence of *Wolbachia* infection in a target area. Additionally, we will try to find both the optimal (minimum) application period and total cost (associated with the number of released mosquitoes) to achieve it. For further details about the calculation of the equilibrium points and their stability (by analytical or numerical techniques), we refer to [24].

3 Feedback Linearization Technique

Essentially, exact feedback linearization relies on algebraically convert the dynamics of a nonlinear system into a (fully or partly) linear system, thus allowing the application of linear control techniques. Compared to the classical Taylor series (or Jacobian) linearization, it has the following advantages:

i. potential global validity, i.e. the linearization holds to the entire state space domain (other than possible singularity points);
ii. feedback and exact state transformations, instead of linear approximations of the system dynamics.

Another important feature of this technique is getting a mathematical expression, depending on some parameters, which may be optimized based on intended objectives (minimizing control cost, application time, or maximizing the system performance, etc.) to obtain an optimal control of the system [26,27].

Feedback linearization may be of two types: input-state and input-output linearization. In this paper, we focus on the input-output linearization of single-input nonlinear systems described by the state space representation

$$\begin{aligned} \dot{\mathbf{x}} &= \mathbf{f}(\mathbf{x}) + \mathbf{g}(\mathbf{x})\, u \\ y &= h(\mathbf{x}) \end{aligned} \tag{3}$$

where $\mathbf{x} \in \mathbb{R}^n$ is the state vector, y is the system output, u is the scalar control input and $\mathbf{f}, \mathbf{g} : D \subseteq \mathbb{R}^n \to \mathbb{R}^n$ are smooth vector fields.

Basically, the input-output linearization entails two steps: (i) to differentiate the output function y repetitively until the input u comes up and (ii) design u in order to remove the nonlinearities. Step (ii) is only possible when the system *relative degree* (r), which stands for the number of differentiations in step (i), is defined. Necessarily, the relative degree does not exceed the system order n, i.e. $r \leq n$, and if $r = n$ the input-output linearization produces an input-state linearization. Remarkably, the input-output technique converts the nonlinear system (3) into a linear observable subsystem and a nonlinear unobservable subsystem (also called

internal dynamics), such that only the former is changed by the control law.

Let us detail what goes on when $r < n$. In the state space, consider a region (an open connected set) $\mathbf{\Omega_x}$. Following the notation of differential geometry, the process of repeated differentiation starts with

$$\dot{y} = \nabla h(\mathbf{f} + \mathbf{g}u) = L_\mathbf{f}\, h(\mathbf{x}) + L_\mathbf{g}\, h(\mathbf{x})\, u$$

where $L_i h,\ i = \{\mathbf{f}, \mathbf{g}\}$, represents the Lie derivative of h with respect to i.

If $L_\mathbf{g}\, h(\mathbf{x}) \neq 0$ for some $\mathbf{x} = \mathbf{x}_0$ in $\mathbf{\Omega_x}$, then, by continuity, that relation is valid in a finite neighborhood $\mathbf{\Omega}$ of $\mathbf{x}_0$. In $\mathbf{\Omega}$, the input transformation

$$u = \frac{1}{L_\mathbf{g}\, h}\left(-L_\mathbf{f}\, h + \nu\right),$$

where ν is the external reference input, results in a linear relation between y and ν, namely $\dot{y} = \nu$.

If $L_\mathbf{g}\, h(\mathbf{x}) = 0$ for all $\mathbf{x}$ in $\mathbf{\Omega_x}$, it is possible to differentiate $\dot{y}$ to get

$$\ddot{y} = L_\mathbf{f}^2\, h(\mathbf{x}) + L_\mathbf{g}\, L_\mathbf{f}\, h(\mathbf{x})\, u.$$

If again $L_\mathbf{g}\, h(\mathbf{x}) = 0$ for all $\mathbf{x}$ in $\mathbf{\Omega_x}$, we shall differentiate again and again

$$y^{(i)} = L_\mathbf{f}^i\, h(\mathbf{x}) + L_\mathbf{g}\, L_\mathbf{f}^{i-1} h(\mathbf{x})\, u$$

until for some r

$$L_\mathbf{g}\, L_\mathbf{f}^{r-1} h(\mathbf{x}) \neq 0.$$

for some $\mathbf{x} = \mathbf{x}_0$ in $\mathbf{\Omega_x}$. Then, by continuity, the above relation is verified in a finite neighborhood $\mathbf{\Omega}$ of $\mathbf{x}_0$. In $\mathbf{\Omega_x}$, the control law

$$u = \frac{1}{L_\mathbf{g}\, L_\mathbf{f}^{r-1}\, h}\left(-L_\mathbf{f}^r\, h + \nu\right) \tag{4}$$

applied to

$$y^{(r)} = L_\mathbf{f}^r\, h(\mathbf{x}) + L_\mathbf{g}\, L_\mathbf{f}^{r-1} h(\mathbf{x})\, u \tag{5}$$

leads to the linear relation

$$y^{(r)} = \nu. \tag{6}$$

Isidori [26] observes that on the linear system thus obtained one can impose the external reference input ν in order to assign a specific set of eigenvalues or to satisfy an optimality criterion.

If r is defined and $r < n$, it is possible to get more formal notions of the internal dynamics and zero-dynamics (see definition later) by transforming the nonlinear system (3) into the so-called "normal form", wherein $y, \dot{y}, \ldots, y^{(r-1)}$ are part of the new state components. Letting

$$\boldsymbol{\mu} = \left[\ \mu_1\ \mu_2\ \cdots\ \mu_r\ \right]^T = \left[\ y\ \dot{y}\ \cdots\ y^{(r-1)}\ \right]^T, \tag{7}$$

in a neighborhood of a point $\mathbf{x}_0$, the normal form may be set as

$$\begin{aligned} \dot{\boldsymbol{\mu}} &= \begin{bmatrix} \mu_2 \\ \cdots \\ \cdots \\ \mu_r \\ a(\boldsymbol{\mu}, \boldsymbol{\Psi}) + b(\boldsymbol{\mu}, \boldsymbol{\Psi})\, u \end{bmatrix} \\ \dot{\boldsymbol{\Psi}} &= \mathbf{w}(\boldsymbol{\mu}, \boldsymbol{\Psi}) \\ y &= \mu_1. \end{aligned} \tag{8}$$

The nonlinear system (3) can only be transformed into the normal form (8) if such a coordinate transformation exists and it is a true state transformation. Equivalently, a (local) diffeomorphism

$$\boldsymbol{\phi}(\mathbf{x}) = \left[\ \mu_1\ \ldots\ \mu_r\ \Psi_1\ \ldots\ \Psi_{n-r}\ \right]^T \tag{9}$$

must be conceivable so that (8) is verified.

An important step is determining the vector field $\boldsymbol{\Psi}$ to complete the transformation into a normal form. This is achieved by solving the following set of partial differential equations in Ψ_j:

$$\nabla \Psi_j\ \mathbf{g} = \frac{\partial \Psi_j}{\partial \mathbf{x}}\mathbf{g} = 0, \quad 1 \leq j \leq n - r, \tag{10}$$

whence it immediately follows that $\boldsymbol{\Psi} := \boldsymbol{\Psi}(\mathbf{x})$ and hence the equations $\dot{\boldsymbol{\Psi}} = \mathbf{w}(\boldsymbol{\mu}, \boldsymbol{\Psi})$ in (8) are ultimately determined by using the system (3) equations.

The internal dynamics in the input-output linearization correspond to the $(n - r)$ equations $\dot{\boldsymbol{\Psi}} = \mathbf{w}(\boldsymbol{\mu}, \boldsymbol{\Psi})$ of the normal form and represent the unobservable dynamics of the system (for more information, see [26,27]).

The effectiveness of the control design relies upon the stability of the internal dynamics, which can be determined more easily by examining the stability of the zero-dynamics, defined to be *the internal dynamics of the system when the system output is kept at zero by the input*. After the normal form (8), the zero dynamics are described by

$$\begin{aligned} \dot{\boldsymbol{\mu}} &= \mathbf{0} \\ \dot{\boldsymbol{\Psi}} &= \mathbf{w}(\mathbf{0}, \boldsymbol{\Psi}). \end{aligned} \tag{11}$$

Although the input-output linearization is motivated in the context of output tracking, it can also be applied to stabilization problems. Let us see how it works in this regard. Assume that in (6) we let

$$\nu = -q_{r-1} y^{(r-1)} - \ldots - q_1 \dot{y} - q_0 y, \tag{12}$$

where the coefficients q_i are chosen such that the polynomial

$$Q(p) = p^r + q_{r-1} p^{r-1} + \ldots.. + q_1 p + q_0 \tag{13}$$

has all its roots strictly in the left-half plane. Then, the actual control input u can be written from (4) as

$$u(\mathbf{x}) = \frac{1}{L_\mathbf{g} L_\mathbf{f}^{r-1} y}\left[-L_\mathbf{f}^r y - q_{r-1} y^{(r-1)} - \ldots - q_1 \dot{y} - q_0 y\right]. \tag{14}$$

Finally, since the zero-dynamics are asymptotically stable, the Slotine theorem [27] ensures that the control law (14) locally stabilizes the whole system.

Next, a control law for the trivial solution is determined by applying the input-state linearization technique to the system (1). A suitable translation of it produces the control law for any non-trivial equilibrium point, what we will do for the coexistence equilibrium point (F_c, W_c).

4 Input-Output Linearization on the system

Setting a system output as a linear combination of the states

$$y = aF + bW, \tag{15}$$

with a and b constants, the mathematical model (1) can be written as

$$\begin{bmatrix} \dot{F} \\ \dot{W} \end{bmatrix} = \begin{bmatrix} f_1(F,W) \\ f_2(F,W) \end{bmatrix} + \mathbf{g}\,u(t), \tag{16}$$

where $\mathbf{g} = [0 \quad 1]^T$.

4.1 Control law for the trivial steady state

By deriving one time ($r = 1$) the output equation (15), the following direct relation between the input u and the output y may be found:

$$\dot{y} = af_1(F,W) + bf_2(F,W) + bu(t). \tag{17}$$

Thus, we determine the control input to locally asymptotically stabilize the system around the origin from the expression which cancels the nonlinearity into (17):

$$u_0 = -\frac{1}{b}\left[af_1(F,W) + bf_2(F,W) - \nu\right], \tag{18}$$

where $\nu = -q_0 y = -q_0(aF + bW)$ and q_0 is properly chosen so that the polynomial $Q(p) = p + q_0$ has negative roots, i.e. $q_0 > 0$.

Now, let us put the system into the normal form and get its internal dynamics.

4.1.1 Normal form of the system

As the relative degree is $r = 1$, the system conversion to the normal form is done by a diffeomorphism (9) whose expression is:

$$\mathbf{\Phi} = \begin{bmatrix} \mu_1 & \Psi_1 \end{bmatrix}^T \tag{19}$$

where $\mu_1 = y$ and Ψ_1 is solution of the partial differential equation (PDE) $\nabla\Psi_1.\boldsymbol{g} = 0$. Among all the possibilities, we will try the simplest assignment $\Psi_1 = F$. Therefore, from (19) and (15):

$$\mathbf{\Phi} = \begin{bmatrix} \mu_1 & \Psi_1 \end{bmatrix}^T = \begin{bmatrix} aF + bW & F \end{bmatrix}^T. \tag{20}$$

By analyzing the Jacobian of (20), we conclude that $\mathbf{\Phi}$ is a diffeomorphism if $a \in \mathbb{R}$, $b \in \mathbb{R}^*$, $\forall F, W$. Moreover, the inverse diffeomorphism is

$$\begin{aligned} F &= \Psi_1, \\ W &= \tfrac{\mu_1 - a\Psi_1}{b}. \end{aligned} \tag{21}$$

Introducing the relations (20)-(21) into (8), we get the normal form to the system (1):

$$\begin{aligned} \dot{\mu_1} &= a\left[\left(\phi_f - \tfrac{r_f}{K_f}\left(\Psi_1 + \tfrac{\mu_1 - a\Psi_1}{b}\right)\right)\Psi_1\left(\tfrac{\Psi_1}{K_0} - 1\right) - \delta_f\Psi_1\right] + \\ &\quad b\left[\left(\phi_w - \tfrac{r_w}{K_w}\left(\Psi_1 + \tfrac{\mu_1 - a\Psi_1}{b}\right)\right)\tfrac{\mu_1 - a\Psi_1}{b} - \delta_w\tfrac{\mu_1 - a\Psi_1}{b} + \right. \\ &\quad \left. u(t)\right], \\ \dot{\Psi_1} &= \left(\phi_f - \tfrac{r_f}{K_f}\left(\Psi_1 + \tfrac{\mu_1 - a\Psi_1}{b}\right)\right)\Psi_1\left(\tfrac{\Psi_1}{K_0} - 1\right) - \delta_f\Psi_1, \\ y &= \mu_1. \end{aligned} \tag{22}$$

4.1.2 Asymptotic stability of the zero dynamics

The zero dynamics result from (22) by assuming $\mu_1 = 0$, $\forall t$:

$$\begin{aligned} \dot{\Psi_1} &= \left(\phi_f - \tfrac{r_f}{K_f}\left(\Psi_1 - \tfrac{a\Psi_1}{b}\right)\right)\Psi_1\left(\tfrac{\Psi_1}{K_0} - 1\right) - \delta_f\Psi_1, \\ y &= 0. \end{aligned} \tag{23}$$

Also, $\Psi_1^* = 0$ is a critical point of the zero dynamics (23) whose characteristic equation is given by:

$$\lambda + \phi_f + \delta_f = 0, \tag{24}$$

with a single eigenvalue

$$\lambda = -(\phi_f + \delta_f). \tag{25}$$

Therefore, the zero dynamics (23) are asymptotically stable around $\Psi_1^* = 0$ if and only if

$$\phi_f, \delta_f > 0, \tag{26}$$

leading to the local asymptotic stability of system (1) around the origin, by the Slotine theorem [27], when the control is applied according to Eq. (18).

4.2 Control law for the nonzero steady state

After translating the coexistence steady state (F_c, W_c) to the origin by the coordinate transformation

$$\begin{aligned} z_1 &= F - F_c, \\ z_2 &= W - W_c, \end{aligned} \tag{27}$$

the control law to locally asymptotically stabilize the populations around (F_c, W_c) is obtained from (18) as

$$u_c = -\frac{a}{b} f_1(z_1+F_c, z_2+W_c) - f_2(z_1+F_c, z_2+W_c) + \frac{\nu}{b}, \quad (28)$$

with

$$\nu = -q_0\,[a(z_1 + F_c) + b(z_2 + W_c)], \;\; q_0 > 0. \quad (29)$$

According to [24], the instantaneous growth of wild females should be negative $\left(\frac{dF}{dt} < 0\right)$ when $F(t) < K_b$ and positive $\left(\frac{dF}{dt} > 0\right)$ when $F(t) > K_b$ (see the corresponding phase diagram in [24], Figure 1 on page 1015). Since the control law (18) is state-dependent and acts directly on the solution component $W(t)$ and not $F(t)$, it may not be sufficiently large to bring the solution to the origin if $F(0) > K_b$. Hence, (28) can fail to drive the solution to the coexistence equilibrium point (F_c, W_c) if the following condition to the system translated by (27) is not fulfilled:

$$\begin{aligned} z_1(0) < K_b &\Longrightarrow F(0) - F(c) < K_b \\ &\Longrightarrow F(0) < F_c + K_b. \end{aligned} \quad (30)$$

For the possible scenario where the wild population is above the threshold $F_c + K_b$, we determined an optimized pattern to release *Wolbachia*-carrying mosquitoes pushing the wild population under it to successfully apply u_c. In the following section, this additional strategy based on a genetic algorithm solution is presented. Firstly, the optimization problem is set up; after, a sub-optimal solution is obtained.

5 Heuristic approach

As discussed earlier, when $F(0) > F_c + K_b$, the u_c-driven control is not able to make the solution converge to the coexistence equilibrium. Thus, we want to find a strategy to lead the solution component $F(t)$ below the threshold $F_c + K_b$. From that point on, the u_c-driven control shall work such as it is meant to do.

Let $u(t)$ be the decision variable describing the number of *Wolbachia*-carriers to be released on a day t at a target locality. Also, $t \in [0, T]$ and $u(t) \in [0, w_{\max}]$, where T is the total amount of days of a control application and $w_{\max}$ is the maximum number of *Wolbachia*-carrying females available for a daily release, naturally depending on the production capacity of a laboratory where *Wolbachia*-carriers are raised. We want to determine $u^*(t)$ which satisfies the optimization problem described below. To solve it, a Genetic Algorithm (GA) is proposed, hence a discretized form is demanded.

$$\textit{Minimize } J = \sum_{t=1}^{T} u(t) \quad (31)$$

Subject to

$$\textit{System (1)} \quad (32)$$
$$F(T) < F_c + K_b \quad (33)$$
$$W(T) < W_c \quad (34)$$
$$F(0) = K_* \quad (35)$$
$$W(0) = 0 \quad (36)$$
$$F(t),\, W(t) \geq 0 \quad (37)$$
$$0 \leq u(t) \leq w_{\max} \quad (38)$$
$$0 \leq t \leq T \quad (39)$$

The functional (31) is related to the control applied in the time interval $[0, T]$. The constraint (34) guarantees positive values of u_c, which will be applied after $u^*(t)$, for $t > T$. If $W(t)$ is smaller than W_c, more individuals are needed to approach W_c, otherwise u_c would assume negative values representing the death of mosquitoes, which is inappropriate after its biological definition as mosquito release. Constraints (35)-(36) correspond to the worst scenario where a wild (*Wolbachia*-free) mosquito population is established in the target area free of *Wolbachia*-carrying individuals [24]. Ultimately, the constraint (37) establishes the non-negativity of the state variables ensuring their biological meaning.

Let us see a brief description of the Genetic Algorithm used for solving the previous problem (a complete explanation of genetic algorithm features may be found in [29]).

5.1 Genetic Algorithm

The metaheuristics Genetic Algorithm is based on Charles Darwin's theory of natural selection and was originally proposed by J. H. Holland in 1992 [30]. In this algorithm, a population of N individuals is created, where each one constitutes a solution of the optimization problem. In general, these individuals are represented by a matrix, the so-called chromosome of the individual. At each generation (iteration), the individuals are evaluated with regard to their fitness (usually based on the cost function) and come across genetic operators which might promote an improvement of solutions: selection, crossover, and mutation. The selection of individuals who will be crossed is performed by a randomized process in which fitter individuals have a higher probability of being chosen. From the several existent methods [31], we used the Tournament Method due to its simplicity, where the fitter of every two individuals randomly taken is chosen and stored in a mating pool. Two individuals (father and mother) from the mating pool are randomly selected for crossover, which generates new individuals (children)

through their genetic combination. Moreover, the individuals have a low probability (usually until 0.05) of undergoing mutation. This process favors population diversity avoiding local convergence. After that, a new population is created composed of the best individuals from the previous population and those from the crossover and mutation processes. In the new population, one or more of the best individuals are to be identified or stored (elite). It has been shown that elitism enables quicker convergence to the global optimal solution [32]. These genetic operators are repeated until a stopping condition is satisfied (time, generation number, etc.). In the end, one chooses the best solution for the final population (from elite) as the solution of the optimization problem. Distinct approaches to genetic operators determine different Genetic Algorithms.

GAs are very efficient in searching for good quality solutions, for a wide variety of optimization problems, because they do not possess many of the limitations found in traditional methods [29]. In fact, GAs do not require a well-behaved objective function, and they can be adapted to produce feasible solutions, thus being suitable to optimization problems with a broad range of objective functions and constraints. They have also the advantage of determining a discretized solution that is well-suited for real-world application, as in the specific case analyzed in this paper.

In this work, we define the chromosome structure of an individual as a vector u with T elements, in which the allele present in the t^{th} gene $u(t)$, $t = 1, ..., T$ represents the amount of control applied on the day t (Figure 1).

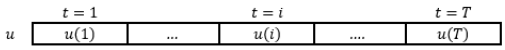

Fig. 1: Chromosome structure used in the GA, representing a *Wolbachia*-based biocontrol strategy to be applied during T days.

The steps followed by the GA are:

1. Define the input parameters: number of generations G, population size N, number L of individuals to be selected (generally $L \leq 0.8N$), mutation probability α (usually $\alpha \leq 0.05$) and the chromosome size T.
2. **Initial Population**: Generate the initial population P with N individuals as shown in Figure 1 and do $P_A \leftarrow P$ (P_A is an auxiliary matrix) .
3. **Evaluation**: assess each individual (ind) of P by its fitness $\mathbb{F}_{ind}$.
4. **Genetic operators**: Repeat G times:
   a) **Selection**: apply the selection criterion to the L individuals to be crossed (tournament method);
   b) **Crossover**: Perform crossover of the L selected individuals as shown in Figure 2 (description below). Store the new individuals in P_A;
   c) **Mutation**: Perform mutation of the chosen individuals for it (explained below) and store the new individuals in P_A. Evaluate all individuals generated through Crossover and Mutation operators according to step 3;
   d) **New Population**: Create a new population P by retaining the N best-fitted individuals from P_A and update P_A: do $P \leftarrow \{\}$, $P \leftarrow \{N$ best individuals from $P_A\}$, $P_A \leftarrow \{\}$ and $P_A \leftarrow P$ in a row. This way of storing the new individuals ensures that elite individuals are not lost.
5. Output: the solution u^* is the best solution of P.

The initial population was randomly generated. Each individual ind was built with one integer w randomly generated in $[0, w_{\max}]$, where $ind = 1, \ldots, N$ and $w_{\max}$ is the maximum number of *Wolbachia*-carrying mosquitoes available for each daily release. In this way, the individuals of the initial population were of the form $u_{ind} = [w, w, ..., w]$. Applying the genetic operators changes the composition of the individuals.

The evaluation of any individual ind was based on the following functional

$$\mathbb{F}_{ind} = J_{ind} + p_{ind}, \ ind = 1, 2, \ldots, N, \qquad (40)$$

where J_{ind} is the value of the functional (31) and p_{ind} penalizes the infeasibility of the individual ind (when it does not satisfy the constraints (33)-(34)).

Selecting was carried out by tournament. The fitter among two randomly selected individuals of P gets in the *Mating Pool*. This process is repeated L times ($L \leq N$).

For crossover, two individuals (parents) from the *Mating Pool* are taken and one draws two random integers for chromosome cut-off points: $r_1 \in [1, T-1]$ and $r_2 \in [r_1, T-1]$. These numbers are used to crossover the genetic charge of parents and generate two new individuals (Figure 2).

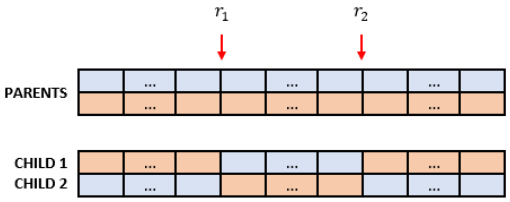

Fig. 2: Two-point crossover process.

As for the mutation operator, the probability of an individual mutating is α (usually $\alpha = 0.05$). A number $r \in [0, 1]$ is drawn and if $r \leq \alpha$ the individual mutates, otherwise nothing changes. To the mutation of the individual u_{ind} one draws three random integer numbers: $r_{ind1} \in [1, T-1]$, $r_{ind2} \in [r_{ind1}, T-1]$ and

$w_{ind} \in [0, w_{\max}]$. Ultimately, the genetic load from r_{ind1} to r_{ind2} is replaced by w_{ind} generating the mutated individual u_{indm} (Figure 3).

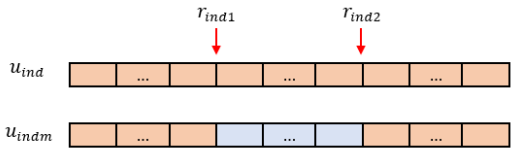

Fig. 3: Mutation process.

The proposed GA was able to determine the sub-optimal control u^* for a given time period T. To minimize T, one suggests studying the trade-off between the objectives of minimizing T and minimizing $J(u,T)$. For this, one fixes ever lower values of T solving the optimization problem (31)-(39) until finding a minimal value T^* to which there exists a solution. This technique is similar to the ϵ-restricted method [33], in which $T \leq \epsilon$ is added to the constraint set, and then one solves the model for fixed values of the upper bound ϵ.

6 Numerical simulations and discussion

To illustrate the proposed methodology, computational tests were carried out aiming to determine a control strategy based on the releasing of *Wolbachia*-carrying mosquitoes ($u(t)$, system (1)) in order to promote the coexistence of both *Wolbachia*-free (wild) and *Wolbachia*-carrying mosquitoes. Following the earlier explanation from Subsection 4.2, there may be two types of strategy depending on the initial size of the wild population $F(0)$:

- *one-control strategy*: if $F(0) < F_c + K_b$, the u_c-driven control (given by equation (28)) is enough to bring the system solution to the coexistence point;
- *two-control strategy*: if $F(0) \geq F_c + K_b$, u^* is applied until $t = T^*$ in order to have $F(T^*) < F_c + K_b$. Then, the u_c-driven control is triggered on.

Table 1 shows the parameter set [24] regarding to *wMelPop* strain for the model (1) and for u_c (given by (28)) used in the simulations; $\phi_f, \phi_w, \delta_f, \delta_w, r_f, r_w$ in $[\text{days}]^{-1}$, and K_f, K_w, K_0 in [individual]. The parameters a, b, and q_0 have no units. For this parameter setting, $F_c = 40.943$, $W_c = 259.06$, $K_b = 33.327$ and $K_* = 413.17$.

To determine u^* and T^*, the optimization model (31)-(39) was solved by using the proposed GA (Section 5), whose parameter values are given in Table 2. The chosen value for the upper bound $w_{\max} = 400$ was never reached.

GNU Octave 6.3.0 was used to solve both the ODE system (1) and the optimization problem (31)-(39).

Table 1: Parameter set [24] for the system (1) and for u_c (28) used in all simulations

Parameter	Range
$\phi_f = 0.32667$	$0.28 - 0.38$
$\phi_w = 0.21333$	$0.18 - 0.25$
$\delta_f = 0.03333$	$1/8 - 1/42$
$\delta_w = 0.06666$	$2/8 - 2/42$
$K_f = 374$	
$K_w = 300$	
$K_0 = 30$	
$a = 0.1$	
$b = 10$	
$q_0 = 0.5$	

Table 2: Parameter set for the GA described in Section 5.1

Parameter	G	N	L	α
Value	50	100	0.8N	0.5

6.1 One-control strategy

Firstly, we illustrate the control law u_c (given by (28)) efficacy to promote alone the asymptotic local stability of the coexistence steady state when $F(0) < F_c + K_b$ (see Subsection 4.2). For an initial wild population $F(0) = F_c + K_b - 1 < F_c + K_b$, Figure 4 (top chart) exhibits the corresponding u_c-driven control suggesting a large release of *Wolbachia*-carrying females on the first days and virtually none from about the 10^{th} day. Figure 4 (bottom chart) shows that with such control, both populations converge to the coexistence steady state (F_c, W_c) just over 20 days.

The shape of the u_c-driven control curve, derived from the asymptotic convergence which it yields, could lead to the misconception that it is possible to permanently stop the intervention at some point. As we shall see, the control may only be interrupted temporarily, but for a considerable time span.

6.2 Two-control strategy

Now, we show the combination of both the sub-optimal u^* and u_c-driven controls to achieve the asymptotic stability of the coexistence equilibrium (F_c, W_c) when $F(0) > F_c + K_b$. Henceforth, we approach the worst scenario expected in nature [24] with the wild female *Aedes aegypti* population at its upmost level $F(0) = K_*$ and no prior *Wolbachia*-carrying individuals. As discussed in Subsection 4.2, just the u_c usage would not work to drive the population to the coexistence equilibrium. Let us see how u^* and T^* are obtained.

6.2.1 Getting u^* and T^* through GA

The minimum application time $T^* = 22$ days was reached by studying the trade-off between minimizing both T and

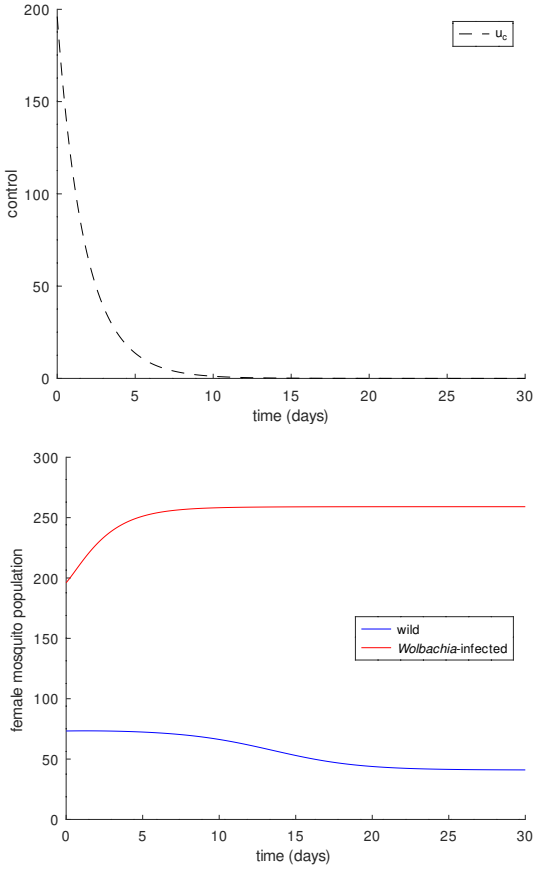

Fig. 4: Temporal evolution of the u_c-driven control (28) accounting for daily releases of *Wolbachia*-carrying individuals *(top)*; trajectories of system (1) under u_c application, given the initial condition $F(0) = F_c + K_b - 1 < F_c + K_b$ and the parameter set displayed in Table 1 *(bottom)*.

$J(u,T)$. The initial value $T = 63$ was reduced until the GA was unable to find a feasible solution to the optimization problem (31)-(39). Interestingly, shorter periods of control application do not imply higher costs, but rather we see a quasi-linear increasing tendency of the total amount of *Wolbachia*-carrying mosquitoes to be released as the time span rises (Figure 5).

Figure 6 shows the convergence study for the metaheuristic GA. It could minimize the functional (31) in 60 generations (iterations). As there was no cost improvement thereafter, the algorithm ceased the search with 100 generations.

For the minimum period $T^* = 22$ days, the sub-optimal solution u^* suggests a massive release of *Wolbachia*-carrying females for three days (2^{nd} to 4^{th}) followed by a sharp control reduction (Figure 7). From day 5, the population dynamics is practically driven by the interaction between infected and non-infected mosquitoes.

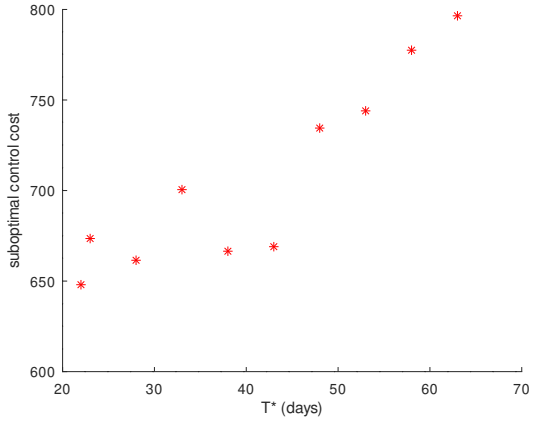

Fig. 5: Cost of the sub-optimal control u^* versus application time (during which the *Wolbachia*-carrying mosquitoes are released). Each point corresponds to the sub-optimal solution obtained via GA algorithm.

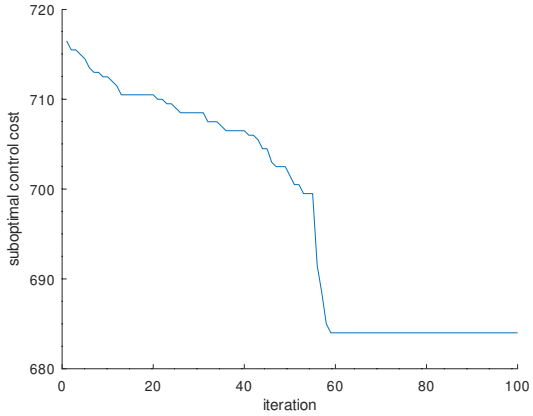

Fig. 6: Sub-optimal Control cost versus iteration of the GA showing its convergence. The system (1) was run from $t = 1$ to $T = 33$ days.

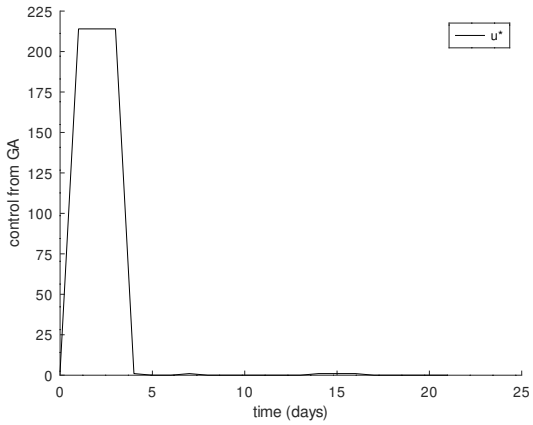

Fig. 7: Sub-optimal control u^* to the optimization problem (31)-(39) for the shortest possible time span $T^* = 22$ days.

While running the GA, one observed a few feasible solutions to the optimization problem (31)-(39). Thus, a sensitivity analysis was performed in order to investigate if small variations in the sub-optimal solution incur a loss of feasibility related to the conditions (33) and (34). The analysis consisted of making randomized perturbations $([u^*(t) - 4, u^*(t) + 4])$ on the values of u^*, $t \in [1, T^*]$, $T^* = 22$ days, and verify the impact in terms of still fulfilling the conditions (33) and (34) (Figure 8).

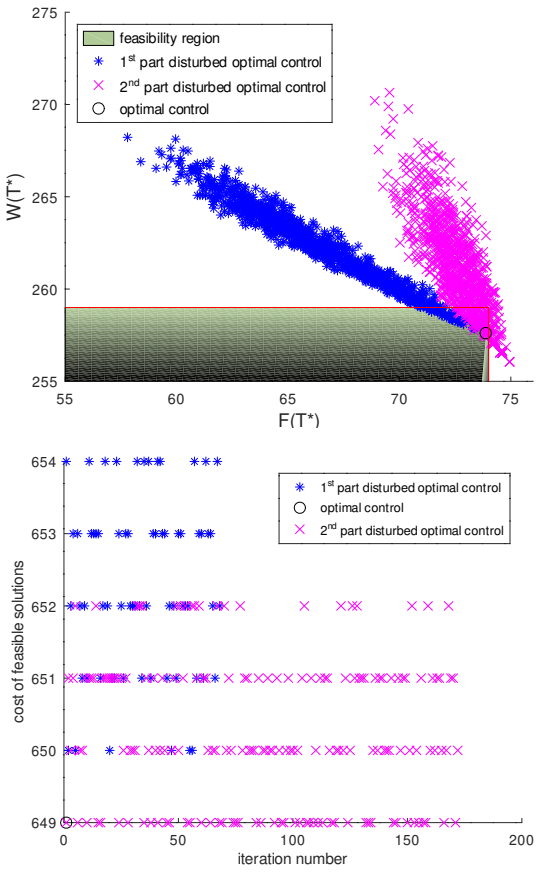

Fig. 8: Sensitivity analysis as for small perturbations in the control u^* and consequent disturbance in meeting the conditions (33) and (34) from the optimization model: feasibility shift due to perturbations in u^* for $t \in [1, 11]$ (blue) and in u^* for $t \in [12, 22]$ (pink) *(top)*; value of $J(u, T^*)$ in which u is a feasible disturbance of u^* *(bottom)*.

Figure 8 (top chart) shows the coordinates $(F(T^*), W(T^*))$ of u^* (sub-optimal control), a part of the feasibility region (which comprises $0 \leq F(T^*) < F_c$ and $0 \leq W(T^*) < F_c$), and the impact of small perturbations in u^* over the solution of the system. We can see that small perturbations in the daily release of *Wolbachia*-carrying mosquitoes cause a great variation in the values of $(F(T^*), W(T^*))$, which might lead the solution to a feasibility loss concerning the conditions (33) and (34) or to an increase of the control cost associated to the functional J. Furthermore, Figure 8 (top chart) suggests that when the perturbations are on the first 11 days, there is a high change in the amount of wild and *Wolbachia*-carrying females at the final time T^*, while perturbations from day 12 to day 22 imply greater variation mainly in *Wolbachia*-carrying females. Figure 8 (bottom chart) indicates that the control cost is greater when perturbations in u^* occur at $t \in [1, 11]$ than at $t \in [12, 22]$, regardless of the iteration number. The fact that all perturbed solutions have a large cost compared to that of u^* indicates that the GA has a good performance in searching for the optimal solution.

Figure 9 (top chart) shows the control strategy composed of the sub-optimal control u^* along 22 days followed by the u_c-driven releases. As we observe in Figure 9 (bottom chart), from about day 45, the u_c-driven control becomes rather low and the solution apparently "stabilizes" at the coexistence point. Both u^* and u_c-driven controls point out a higher intensity at the beginning of their respective applications, while much less effort is needed at any other moment.

6.3 General remarks

In both presented cases, it is important to highlight that if the u_c-driven control is disabled at a time t the solution shall converge to $(K_*, 0)$ since $F(t) \approx F_c > K_b$ and $W(t) \approx W_c \approx K_w$ [24]. Retaking the scenario in Figure 9, we stopped the u_c-driven control from day 51 and the solution slowly converged to this point (Figure 10).

Remarkably, after being close to the coexistence equilibrium (F_c, W_c) one may turn off and on the u_c-driven control without leaving the feasibility region (Figure 8) wherein u_c application is effective (Figure 11). For the parameter set used, the u_c-driven control could be turned off for a maximum of 44 days (from 51^{th} to 94^{st} day) having to be retaken from then on (Figure 11). This on-off process seems to be an attractive cost-saving characteristic of our control strategy, mainly because when the u_c-driven control is reactivated, low and short-term releases are needed to keep the population size close to the coexistence equilibrium.

In conclusion, the proposed control strategy is quite appealing from a practical point of view because it consists in releasing *Wolbachia*-carrying mosquitoes in larger amounts in the first days, significantly reducing them as the solution approaches the coexistence point. Afterward, the control can be interrupted temporarily, reducing the costs to zero for a substantial length of time. Differently from the approach of [24], we dealt with the coexistence of both wild and *Wolbachia*-carrying populations, providing through the feedback linearization technique a way to achieve it, instead of replacing the wild population by *Wolbachia*-carrying mosquitoes. Even though there is no attested evidence that *Wolbachia*-carrying mosquitoes may induce damage to

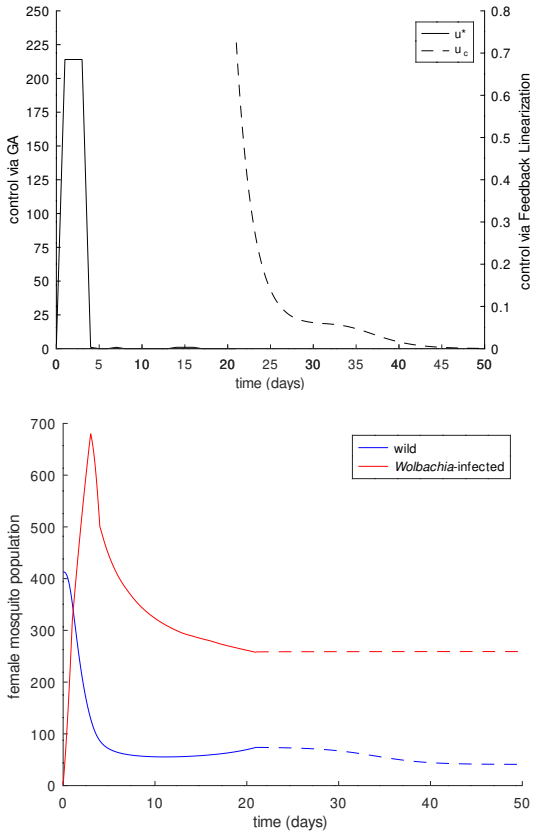

Fig. 9: Temporal evolution of both u^* (continuous line) and u_c-driven controls (dashed line) *(top)*; trajectories of system (1) for the initial condition $F(0) = K_*$, under application of the sub-optimal control u^* for $t \in [0, T^*]$, $T^* = 22$, (continuous line), and the control law u_c (28) from $t = T^*$ on (dashed line) *(bottom)*. Parameter values were taken from Table 1.

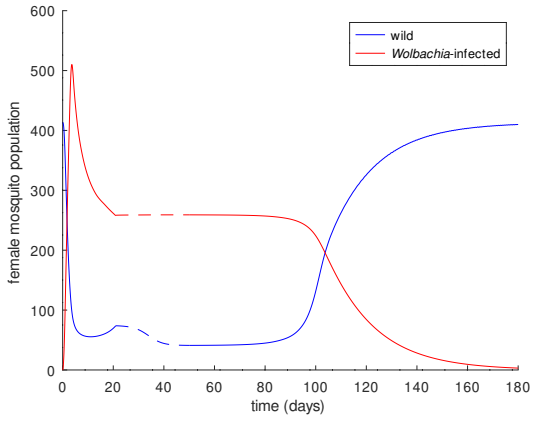

Fig. 10: Trajectories of system (1) under application of the sub-optimal control u^* (continuous line) for $t \in [0, T^*]$, $T^* = 22$, and under the control law u_c (28) (dashed line) from $t = T^*$ to $t = 50$, when the u_c-driven control is turned off.

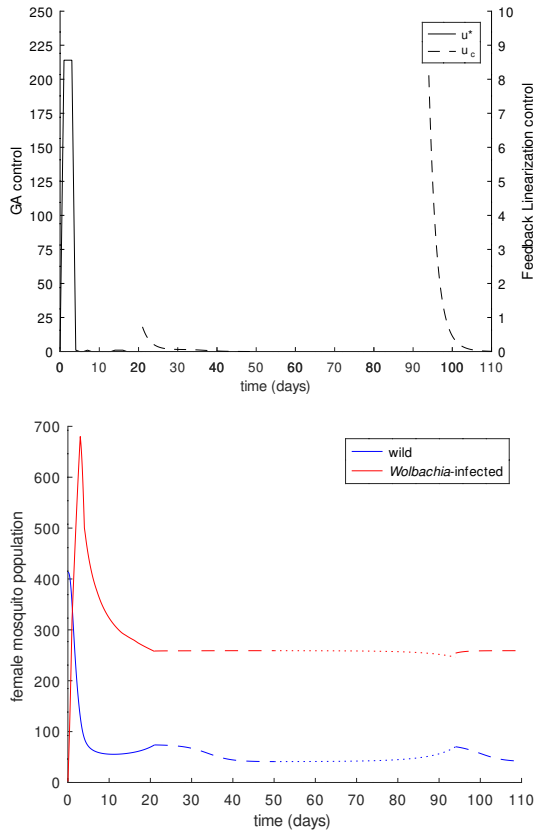

Fig. 11: Temporal evolution of both u^* (continuous line) and u_c-driven (dashed line) controls. The initial conditions are: $F(0) = K_*, W(0) = 0$, and the parameters' values were taken from Table 1 *(top)*; trajectories of system (1) for the initial condition $F(0) = K_*$ under application of the sub-optimal control u^* for $t \in [0, T^*]$, $T^* = 22$, (continuous line), and the control law u_c (28) for both $t \in (T^*, 50]$ and from $t = 95$ on (dashed line); no control was applied for $t \in [51, 94]$ (dotted line) *(bottom)*.

the local ecosystems, such evidence may appear in the future. In this context, the control method proposed here looks more worthwhile, since it allows the recovery of the wild mosquito population, unlike the technique proposed in [24], which guarantees a complete population replacement.

A limitation of the work proposed here is that the discussed control is based on time-continuous application. More realistic implementations of the feedback linearization control law might be investigated by considering discrete time, piecewise, or impulse functions, for example. We intend to explore these possibilities in future work.

7 Conclusion

This work readdressed a mathematical model describing the population dynamics of *Aedes aegypti* composed by

Wolbachia-free and *Wolbachia*-carrying individuals. In the original paper [24], the equilibrium points and their stability were performed, but the unstable steady state of coexistence of the aforementioned populations was not explored by the authors in their optimal control approach. With this in view, our main goal was to design a control intervention policy that relies on daily releases of *Wolbachia*-carrying females, promoting within the shortest possible period of time the invasion and persistence of *Wolbachia*, and the coexistence of both populations of *Aedes aegypti* mosquitoes. For this, a generic control law was designed to assure the stabilization of the coexistence equilibrium point through the feedback linearization technique. The control represents the number of *Wolbachia*-carriers to be released on a given day at a target locality. Depending on the number of *Wolbachia*-free mosquitoes, an additional control, obtained here through a Genetic Algorithm, should be applied before the control law implementation. Remarkably, the presented strategy is rather attractive because it consists in applying the control with higher intensity in the first days and fairly low as the solution approaches the coexistence point. Furthermore, the control can be temporarily interrupted, reducing the costs to zero for a considerable length of time. The results of the computer simulations suggest that the presented methodology has great potential as a tool for decision-makers to keep the wild *Aedes aegypti* population size at an acceptable level, hence containing the transmission of arboviral diseases by this species.

Acknowledgement

This study was supported by São Paulo Research Foundation (FAPESP) [grants #2021/03039-1, #2013/07375-0, #2022/10964-0 and #2019/22157-5] and the National Council for Scientific and Technological Development (CNPq) [grants #306518/2022-8 and #302984/2020-8]. The authors are grateful to the anonymous referees for a careful checking of the details and for helpful comments that improved this paper.

References

[1] K. M. Lizzi, W. A. Qualls, S. C. Brown, and J. C. Beier, Expanding integrated vector management to promote healthy environments, *Trends Parasitol.*, **30**(8), 394–400 (2014).

[2] J. Pretty and Z. P. Bharucha, Integrated pest management for sustainable intensification of agriculture in Asia and Africa, *Insects*, **6**(1), 152–182 (2015).

[3] T. Chareonviriyaphap, M. J. Bangs, W. Suwonkerd, M. Kongmee, V. Corbel, and R. Ngoen-Klan, Review of insecticide resistance and behavioral avoidance of vectors of human diseases in Thailand, *Parasites Vectors*, **6**(1), 1–28 (2013).

[4] A. Philbert, S. L. Lyantagaye, and G. Nkwengulila, A review of agricultural pesticides use and the selection for resistance to insecticides in malaria vectors, *Adv Entomol.*, **2**, 120–128 (2014).

[5] A. Rivero, J. Vezilier, M. Weill, A. F. Read, and S. Gandon, Insecticide control of vector-borne diseases: when is insecticide resistance a problem?, *PLoS Pathog.*, **6**(8), e1001000 (2010).

[6] A. L. Wilson, O. Courtenay, L. A. Kelly-Hope, T. W. Scott, W. Takken, S. J. Torr, and S. W. Lindsay, The importance of vector control for the control and elimination of vector-borne diseases, *PLOS Negl. Trop. Dis.*, **14**(1), e0007831 (2020).

[7] T. Iwamura, A. Guzman-Holst, and K. A. Murray, Accelerating invasion potential of disease vector *Aedes aegypti* under climate change, *Nat. Commun.*, **11**(1), 1–10 (2020).

[8] T. N. Pereira, F. D. Carvalho, S. F. De Mendonça, M. N. Rocha, and L. A. Moreira, Vector competence of *Aedes aegypti*, *Aedes albopictus*, and *Culex quinquefasciatus* mosquitoes for mayaro virus, *PLOS Negl. Trop. Dis.*, **14**(4), e0007518 (2020).

[9] J. A. Souza-Neto, J. R. Powell, and M. Bonizzoni, *Aedes aegypti* vector competence studies: A review, *Infect. Genet. Evol.*, **67**, 191–209 (2019).

[10] N. L. Achee, J. P. Grieco, H. Vatandoost, G. Seixas, J. Pinto, L. Ching-NG, A. J. Martins, W. Juntarajumnong, V. Corbel, C. Gouagna, J.-P. David, J. G. Logan, J. Orsborne, E. Marois, G. J. Devine, and J. Vontas, Alternative strategies for mosquito-borne arbovirus control, *PLOS Negl. Trop. Dis.*, **13**(1), e0006822 (2019).

[11] L. R. Bowman, S. Donegan, and P. J. McCall, Is dengue vector control deficient in effectiveness or evidence?: Systematic review and meta-analysis, *PLOS Negl. Trop. Dis.*, **10**(3), e0004551 (2016).

[12] D. Roiz, A. L. Wilson, T. W. Scott, D. M. Fonseca, F. Jourdain, P. Müller, R. Velayudhan, and V. Corbel, Integrated Aedes management for the control of Aedes-borne diseases, *PLOS Negl. Trop. Dis.*, **12**(12), e0006845 (2018).

[13] P. Gao, E. Pilot, C. Rehbock, M. Gontariuk, S. Doreleijers, L. Wang, T. Krafft, P. Martens, and Q. Liu, Land use and land cover change and its impacts on dengue dynamics in China: A systematic review, *PLOS Negl. Trop. Dis.*, **15**(10), e0009879 (2021).

[14] D. J. Gubler, Dengue, urbanization and globalization: the unholy trinity of the 21st century, *Trop Med Health*, **39**(4SUPPLEMENT), S3–S11 (2011).

[15] S. A. Lee, T. Economou, R. de Castro Catão, C. Barcellos, and R. Lowe, The impact of climate suitability, urbanisation, and connectivity on the expansion of dengue in 21st century Brazil, *PLOS Negl. Trop. Dis.*, **15**(12), e0009773 (2021).

[16] N. L. Achee, F. Gould, T. A. Perkins, R. C. Reiner Jr, A. C. Morrison, S. A. Ritchie, D. J. Gubler, R. Teyssou, and T. W. Scott, A critical assessment of vector control for dengue prevention, *PLOS Negl. Trop. Dis.*, **9**(5), e0003655 (2015).

[17] M. Sicard, M. Bonneau, and M. Weill, *Wolbachia* prevalence, diversity, and ability to induce cytoplasmic incompatibility in mosquitoes, *Curr. Opin. Insect Sci.*, **34**, 12–20 (2019).

[18] C. C. Correa and J. Ballard, *Wolbachia* associations with insects: winning or losing against a master manipulator, *Front. Ecol. Evol.*, **3**, 153 (2016).

[19] I. Iturbe-Ormaetxe, T. Walker, and S. L. O'Neill, *Wolbachia* and the biological control of mosquito-borne disease, *EMBO Rep.*, **12**(6), 508–518 (2011).
[20] J. Dianavinnarasi, R. Raja, J. Alzabut, M. Niezabitowski, and O. Bagdasar, Controlling *Wolbachia* Transmission and Invasion Dynamics among *Aedes aegypti* Population via Impulsive Control Strategy, *Symmetry*, **13**(3) (2021).
[21] B. Zheng and Y. Xiao, A Mathematical Model to Assess the Effect of the Constant Release Policy on Population Suppression, *Nonlinear Anal. Differ. Equ.*, **5**(4), 197–207 (2017).
[22] L. Almeida, Y. Privat, M. Strugarek, and N. Vauchelet, Optimal Releases for Population Replacement Strategies: Application to *Wolbachia*, *SIAM J. Math. Anal.*, **51**, 3170–3194 (2019).
[23] P.-A. Bliman, M. Aronna, F. Coelho, and M. Silva, Ensuring successful introduction of *Wolbachia* in natural populations of *Aedes aegypti* by means of feedback control, *J. Math. Biol.*, **76** (2018).
[24] D. E. Campo-Duarte, D. Cardona-Salgado, and O. Vasilieva, Establishing *wMelPop Wolbachia* Infection among Wild *Aedes aegypti* Females by Optimal Control Approach, *Appl. Math. Inf. Sci.*, **11**, 1011–1027 (2017).
[25] D. E. Campo-Duarte, O. Vasilieva, D. Cardona-Salgado, and M. M. Svinin, Optimal control approach for establishing *wMelPop Wolbachia* infection among wild *Aedes aegypti* populations, *J. Math. Biol.*, **76**, 1907–1950 (2018).
[26] A. Isidori, *Nonlinear Control Systems*, Springer London, London, (1995).
[27] J. Slotine and W. Li, *Applied Nonlinear Control*, Prentice-Hall, New Jersey, (1991).
[28] C. A. Reis, H. de O. Florentino, D. Cólon, S. R. F. Rosa, and D. R. Cantane, An approach of the exact linearization techniques to analysis of population dynamics of the mosquito *Aedes aegypti*, *Math. Biosci.*, **299**, 51–57 (2018).
[29] D. Goldberg, *Design of innovation: Lessons from and for competent genetic algorithms*, Kluwer Academic Publishers, Boston, (2002).
[30] J. H. Holland, Genetic Algorithms, *Sci. Am.*, **267**(1), 66–73 (1992).
[31] K. Jebari, Selection methods for genetic algorithms, *Int. J. Emerg. Sci.*, **3**, 333–344 (2013).
[32] D. Bhandari, C. A. Murthy, and S. K. Pal, Genetic algorithm with elitist model and its convergence, *Int. J. Pattern Recognit. Artif. Intell.*, **10**(6), 731–747 (1996).
[33] K. Deb, *Multiobjective Optimization Using Evolutionary Algorithms*, Wiley, New York, (2001).

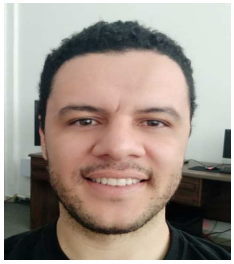

Antone dos Santos Benedito holds a PhD in Biometry from Unesp, Brazil, wherein he is currently developing a postdoctoral research on optimization of *Aedes aegypti* control strategies. His latest interests are in the fields of applied mathematics and optimization, including mathematical models for biological systems, exact and heuristic methods and the feedback linearization technique.

Claudia Pio Ferreira holds a PhD in Physics from USP. Currently, she is a Full Professor at Unesp. She works mainly on Biomathematics and Biological Physics. Her interests are application and development of tools from mathematics, computation, physics and statistics to understand complex systems.

Helenice de Oliveira Florentino Silva received the B.S. degree in Mathematics from Universidade Federal de Uberlândia-UFU, Uberlândia MG, Brazil in 1987. Received the M.S. degree in Computational Mathematics and PhD in Electrical engineering from Universidade do Estado de São Paulo –USP, Brazil, in 1990 and 1997, respectively. From 1990 to today's date, she is Professor of Mathematics in Universidade Estadual Paulista-UNESP. She is Chair of the Operational Research Group. She is involved in research, teaching, and course development in Optimization Theory. Her main area of research is the Multiobjective Optimization Theory.